FireFly: A Time Synchronized Real-Time Sensor Networking Platform

Anthony Rowe, Rahul Mangharam and Raj Rajkumar
Department of Electrical and Computer Engineering
Carnegie Mellon University, Pittsburgh, PA, USA
{agr, rahulm, raj}ece.cmu.edu

1. Introduction

Networks of embedded wireless nodes provide a versatile platform for applications in industrial control, surveillance and inventory tracking. Many of these applications are time sensitive in nature. For cost-effective operation, such nodes feature low-power radios requiring data to be delivered across multiple hops over a wireless interface to one or more destinations. In many applications, nodes must be battery-powered and hence require energy efficient communication. In this chapter we will focus on using time synchronization to provide real-time and energy efficient multi-hop wireless communication. Time synchronization enables the construction of efficient and robust mesh networks for a large class of applications ranging from observation of sporadic events within sensor networks to real-time communication within tightly-coupled control loops.

Time Synchronization in the wireless multi-hop domain provides the following benefits:

1. Energy Efficient Communication. An effective approach to energy-efficient service for applications with either periodic or aperiodic flows is to operate all nodes at low duty cycles so as to maximize the shutdown intervals between packet exchanges. Time synchronization is important because it tightly packs the activity of all nodes so that they may maximize a common sleep interval between activities. Contention based MAC protocols suffer from nearby nodes overhearing packets that are not addressed to them. In a time synchronized network, nodes can be scheduled such that even though they could physically communicate with each other, the topology is logically pruned to avoid it.

2. Bounded Message Latency. Time synchronization allows messages can be scheduled such that they are collision-free. This provides guarantees on timeliness eliminating ambiguity about whether or not a message was dropped or simply delayed. This is important for latency sensitive applications such as control automation systems or interactive media streaming applications.

3. High Throughput. A tightly scheduled collision free environment allows for higher throughput than a system using a contention based scheme. In the wireless sensor network setting this accommodates on-demand bulk transfers of data such as firmware updates, logged sensor data or streaming of high data rate sensors.

4. Deterministic Lifetime. The energy required to power sensor network radios is typically 10 to 20 times more than the underlying CPU power. Since all communication is scheduled in advanced, time synchronization enables the vast majority of energy consumption to be allocated in advanced. Later in the chapter we will discuss how resource reservations can further refine the deterministic lifetime of these systems by managing other energy consuming resources.

5. Total Event Ordering. Many applications such as localization and tracking require ordering of event

	Power	Energy
CPU		$(0.05mW * t_{idle}) + (24.0mW * t_{active})$
Idle	$0.05mW$	$0.05mW * t_{idle}$
Active	$24.0mW$	$24.0mW * t_{active}$
Network		$(.06mW * t_{idle}) + (1.8uJ * N_{rx\_bytes}) + (1.6uJ * N_{tx\_bytes})$
RX	$59.1mW$	$1.8uJ$ per byte
TX	$52.1mW$	$1.6uJ$ per byte
Idle	$.06mW$	$.06mW * t_{idle}$
Sensor		
Light, Temp	$.09mW$	$11.25nJ$ per reading
Microphone	$2.34mW$	$2.87uJ$ per reading
PIR	$5.09mW$	$1uJ$ per reading
Accel	$1.8mW$	$11.25nJ$ per reading

Table 1: Energy statistics for current hardware setup.

samples taken from different nodes at different times. Network wide time synchronization greatly simplify this process by providing absolute time stamps that can be compared against each other.

FireFly is a platform with an accompanying software infrastructure that provides hardware assisted time synchronization, a Time Division Multiple Access (TDMA) MAC protocol, RT-Link, for communication and a reservation based real-time operating system (RTOS), nano-RK, for timely task processing. We have successfully deployed the FireFly sensor platform in various environments. In particular we will discuss our experiences deploying a network within a coal mine for location tracking as well as emergency voice communication.

2. FireFly Hardware Platform

We developed a low-cost low-power hardware platform called FireFly as shown in Figure 1. The board uses an Atmel Atmega32L [1] 8-bit microcontroller and a Chipcon CC2420 [2] IEEE 802.15.4 wireless transceiver. The microcontroller operates at 8Mhz and has 32KB of ROM and 2KB of RAM. The FireFly board includes light, temperature, audio, dual-axis acceleration and passive infrared motion sensors. We have also developed a lower-cost version of the board called the FireFly Jr. that does not include sensors, and is used to forward packets in the network or can be used as a module inside other devices such as actuators that do not require sensing. The FireFly boards can interface with a computer using an external USB dongle.

Table 1 shows a breakdown of the typical energy consumption of the different components on the FireFly board. Since the transmit energy on the boards is quite low (1mW), the analog components in the radio's power amplifier are not as dominant as they would be in other forms of radio like 802.11. This accounts for why the radio receive energy is greater than the transmit energy and means that nodes should not only try to minimize packet transmission, but they should minimize listening time.

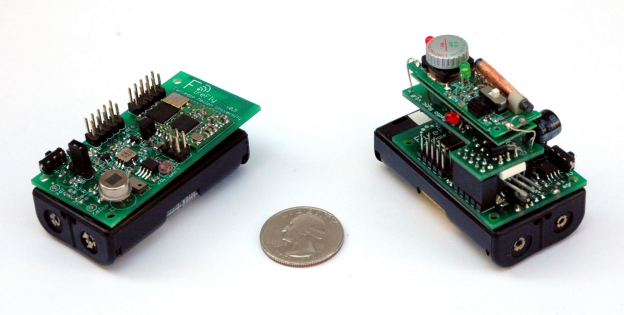

Figure 1: FireFly and FireFly Jr board with AM synchronization module

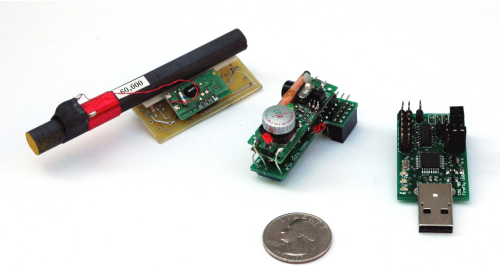

Figure 2: Left to Right: WWVB atomic clock receiver, AM receiver and USB interface board.

2.1. Hardware Assisted Time Synchronization

In order to achieve the highly accurate time synchronization required for TDMA at a packet level granularity, we use two out-of-band time synchronization sources. One uses the WWVB atomic clock broadcast, and the other relies on a carrier-current AM transmitter. In general, the synchronization device should be low power, inexpensive, and consist of a simple receiver. The time synchronization transmitter must be capable of covering a large area.

The WWVB atomic broadcast is a pulse width modulated signal with a bit starting each second. Our system uses an off-the-shelf WWVB receiver (Figure 2) to detect these rising edges, and does not need to decode the entire time string. When active, the board draws 0.6mA at 3 volts and requires less than 5uA when powered off. Inside buildings, atomic clock receivers are typically unable to receive any signal, so we use a carrier-current AM broadcast. Carrier-current uses a building's power infrastructure as an antenna to radiate the time synchronization pulse. We used an off-the-shelf low-power AM transmitter and power coupler [3] that adhere to the FCC Part 15 regulations without requiring a license. The transmitter provides time synchronization to two 5-storey campus buildings which operate on 2 AC phases. Figure 2 shows an add-on AM receiver module capable of decoding our AM time sync pulse. We use a commercial AM receiver module and then designed a custom supporting-board which thresholds the demodulated signal to decode the pulse. The supporting AM board is capable of controlling the power to the AM receiver.

The energy required to activate the AM receiver module and to receive a pulse is equivalent to sending one and a half 802.15.4 packets. The use of a more advanced custom radio solution would bring these values lower and allow for a more compact design. We estimate that using a single chip AM radio receiver, the synchronization energy cost would be less then sending a single in band packet.

In order to maintain scalability across multiple buildings, our AM transmitter locally rebroadcasts the atomic clock time signal. The synchronization pulse for the AM transmitter is a line-balanced 50us square wave generated by a modified FireFly node capable of atomic clock synchronization.

We evaluated the effectiveness of the synchronization by placing five nodes at different points inside an

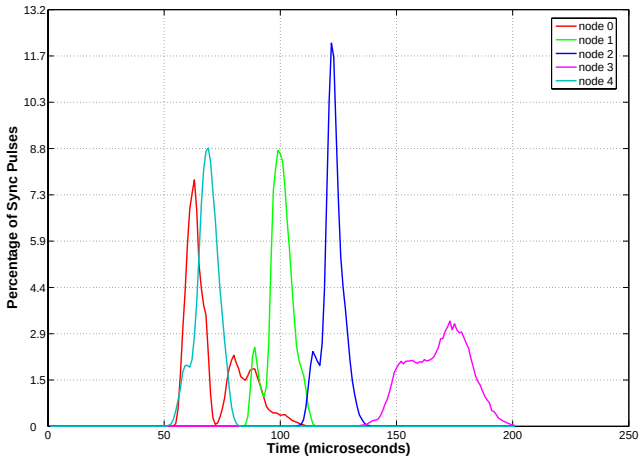

Figure 3: Distributions of AM carrier current time synchronization jitter over a 24 hour period.

8 story building. Each node was connected to a data collection board using several hundred feet of cables. The data collection board timed the difference between when the synchronization pulse was generated and when each node acknowledged the pulse. This test was performed while the MAC protocol was active in order to get an accurate idea of the possible jitter including MAC related processing overhead. Figure 3 shows a histogram with the distribution of each node's synchronization time jitter. An AM pulse was sent once per second for 24 hours during normal operation of a classroom building. The graph shows that the jitter is bounded to within 200us. 99.6% of the synchronization pulses were correctly detected. We found that with more refined tuning of the AM radios, the jitter could be bounded to well within 50us.

In order to maintain synchronization over an entire TDMA cycle duration, it is necessary to measure the drift associated with the clock crystal on the processor. We observed that the worst of our clocks was drifting by 10us/s giving it a drift rate of 10e-5. Our previous experiment illustrates that the jitter from AM radio was at worst 100us indicating that the drift would not become a problem for at least 10 seconds. The drift due to the clock crystal was also relatively consistent, and hence could be accounted for in software by timing the difference between synchronization pulses and performing a clock-rate adjustment. In our final implementation we are able to maintain globally synchronization to within 20us.

3. RT-Link: A TDMA Link Layer Protocol for Multi-hop Wireless Networks

RT-Link is a TDMA-based link layer protocol designed for networks that require predictability in throughput, latency and energy consumption. All packet exchanges occur in well-defined time slots. Global time sync is provided to all fixed nodes by a robust and low-cost out-of-band channel. We now describe in detail the RT-Link protocol, packet types, supported node types and the protocol operation modes.

3.1. Current MAC Protocols

Several MAC protocols have been proposed for low-power and distributed operation for single and multi-hop wireless mesh networks. Such protocols may be categorized by their use of time synchronization as asynchronous, loosely synchronous and fully synchronized protocols. In general, with a greater degree of synchronization between nodes, packet delivery is more energy-efficient due to the minimization of idle listening when there is no communication, better collision avoidance and elimination of overhearing of neighbor conversations. We briefly review key low-power link protocols based on their support for low-power listen, multi-hop operation with hidden terminal avoidance, scalability with node degree and offered

load.

3.1.1. Asynchronous Link Protocols

The Berkeley MAC (B-MAC) [4] protocol performs the best in terms of energy conservation and simplicity in design. B-MAC supports carrier sense multiple access (CSMA) with low power listening (LPL) where each node periodically wakes up after a sample interval and checks the channel for activity for a short duration of 2.5ms. If the channel is found to be active, the node stays awake to receive the payload following an extended preamble. Using this scheme, nodes may efficiently check for neighbor activity. For each transmission instance, the transmitter must remain active for the duration of the receiver's channel check interval. This creates a major drawback since it forces the receiver to check the channel very often (in milliseconds) even when the event sample interval spans several seconds or minutes. For example, if an event occurs ever 20 minutes, all B-MAC receivers check the channel for activity approximately every 80ms to limit the transmitter's burst duration to 80ms [4]. This coupling of the receiver's sampling interval and the duration of the transmitter's preamble severely restricts the scalability of B-MAC when operating in dense networks and across multiple hops. B-MAC does not inherently support collision avoidance due to the hidden terminal problem and the use of RTS-CTS handshaking with LPL is inefficient because the RTS must use the extended preamble. In a multi-hop network, it is necessary to use topology-aware packet scheduling for collision avoidance. Furthermore, upon wake up, B-MAC employs CSMA which is prone to wasting energy and adds non-deterministic latency due to packet collisions.

3.1.2. Loosely Synchronous Link Protocols

Protocols such as S-MAC [5] and T-MAC [6] employ local sleep-wake schedules know as *virtual clustering* between node pairs to coordinate packet exchanges while reducing idle operation. Both schemes exchange synchronizing packets to inform their neighbors of the interval until their next activity and use CSMA prior to transmissions. As all the neighbors of a node cannot hear each other, each node must set multiple wakeup schedules for different groups of neighbors. The use of CSMA and loose synchronization trades energy consumption for simplicity. WiseMAC [7], is an iteration on Aloha designed for downlink communication from infrastructure nodes and has been shown to outperform 802.15.4 for low traffic loads. WiseMAC, however, does not support multiple hop communication. Both T-MAC and WiseMAC use preamble sampling to minimize receive energy consumption during channel sampling. The use of CSMA in each scheme degrades performance severely with increasing node degree and traffic.

3.1.3. Fully Synchronized Link Protocols

TDMA protocols such as TRAMA [8] and LMAC [9] are able to communicate between node pairs in dedicated time slots. TRAMA supports both scheduled slots and CSMA-based contention slots for node admission and network management. LMAC describes a light-weight bit-mask schedule reservation scheme and establishes collision-free operation by negotiating non-overlapping slot across all nodes within the 2-hop radius. Both protocols assume the provision of global time synchronization but consider it an orthogonal problem. RT-Link has similar support for contention slots but employs Slotted-ALOHA [10] rather than CSMA as it is more energy efficient with LPL. Furthermore, RT-Link integrates time synchronization within the protocol and also in the hardware specification. RT-Link has been inspired by dual-radio systems such as [11, 12] used for low-power wake-up. However neither system has been used for time synchronized operation. Several in-band software-based time synchronization schemes such as RBS [13], TPSN [14] and FTSP [15] have been proposed and provide good accuracy. In [16], Zhao provides experimental evidence showing that over one-third of the population of immobile nodes in an indoor environment routinely suffer a link error rate over 50% even when the receive signal strength is above the sensitivity threshold. This severely limits the diffusion of in-band time sync updates and hence reduces the network performance. RT-Link employs an out-of-band time synchronization mechanism which also globally synchronizes all

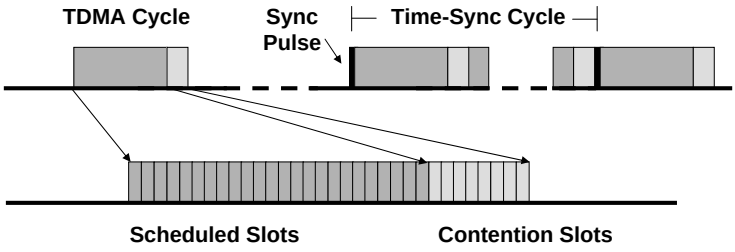

Figure 4: RT-Link time slot allocation with out-of-band synchronization pulses

nodes and is less vulnerable than the above schemes. We believe that hardware-based time sync adds new properties to wireless sensor networks and warrants exploration in a practical environment.

RT-Link supports two node types: fixed and mobile. Both node types include a microcontroller, 802.15.4 transceiver and multiple sensors and are described in detail in Section 2. The fixed nodes have an add-on time sync module which is normally a low-power radio receiver designed to detect a periodic out-of-band global signal. In our implementation, we designed an AM/FM time sync module for indoor operation and an atomic clock receiver for outdoors. For indoors, we use a carrier-current AM transmitter [3] which plugs into the power outlet in a building and uses the building's power grid as an AM antenna to radiate the time sync pulse. We feed an atomic clock pulse as the input to the AM transmitter to provide the same synchronization regime for both indoors and outdoors. The time sync module detects the periodic sync pulse and triggers an input pin in the microcontroller which updates the local time. As shown in Figure 4, this marks the beginning a finely slotted data communication period. The communication period is defined as a fixed-length cycle and is composed of multiple frames. The sync pulse serves as an indicator of the beginning of the cycle and the first frame. Each frame is divided into multiple slots, where a slot duration is the time required to transmit a maximum sized packet. RT-Link supports two kinds of slots: Scheduled Slots (SS) within which nodes are assigned specific transmit and receive time slots and (b) a series of unscheduled or Contention Slots (CS) where nodes, which are not assigned slots in the SS, select a transmit slot at random as in slotted-Aloha. Nodes operating in SS are provided timeliness guarantees as they are granted exclusive access of the shared channel and hence enjoy the privilege of interference-free and hence collision-free communication. While the support of SS and CS are similar to 802.15.4, RT-Link is designed for operation across synchronized multi-hop networks. After an active slot is complete, the node schedules its timer to wake up just before the expected time of next active slot and promptly switches to sleep mode. In our default implementation, each cycle consists of 32 frames and each frame consists of 32 5ms slots. Thus, the cycle duration is 5.12sec and nodes can choose one or more slots per frame up to a maximum of 1024 slots every cycle. The common packet header includes a 32-bit transmit and 32-bit receive bit-mask to indicate during which slots of a node is active. RT-Link supports 5 packet types including HELLO, SCHEDULE, DATA, ROUTE and ERROR. The packet types and their formats are described in detail in [17].

3.2. Network Operation Procedures

RT-Link operates on a simple 3-state state machine as shown in Figure 5. In general, nodes operating in the CS are considered Guests, while nodes with scheduled slots are considered Members of the network. When a fixed node is powered on, it is first initialized as a Guest and operates in the CS. It initially keeps its sync radio receiver on until it receives a sync pulse. Following this, it waits for a set number of slots (spanning the SS) and then randomly selects a slot among the CS to send a HELLO message with its node

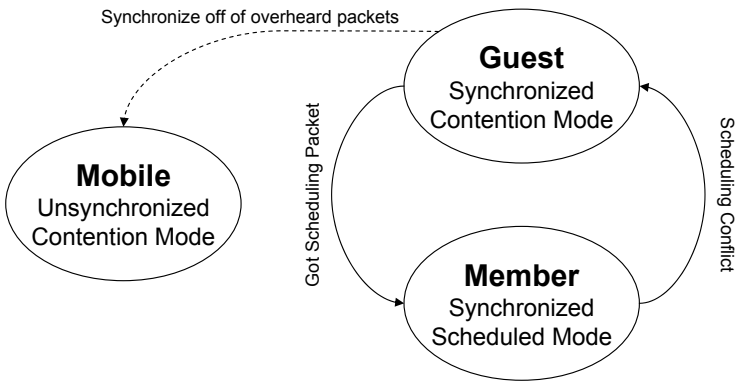

Figure 5: RT-Link node state machine.

ID. This message is then forwarded (via flooding if explicit routes are not present) to the gateway and the node is eventually scheduled a slot in the SS. On the other hand, when a mobile node needs to transmit, it first stays on until it overhears a neighbor operate in an SS. The mobile node achieves synchronization by observing the Member's slot number and computes the time until the start of the CS. Mobile nodes are never made members because their neighborhood changes more frequencty and hence remain silent until a Member provides it a time reference. All nodes with scheduled slots listen on every slot in the CS using LPL. When a node chooses to leave the network, it ceases broadcasting HELLO packets and is gracefully evicted from the neighbor list from each of its neighbors. The gateway eventually detects the absence of the departed node from each of the neighbors' HELLO updates and may reschedule the network if necessary.

For fixed nodes that are unable to receive the global time beacon and for mobile nodes, RT-Link provides software-based in-band time sync. Nodes can implicitly pass time synchronization onto another node using the current slot in the packet header. This implicit time synchronization can cascade across multiple hops.

3.3. Logical Topology Control

RT-Link schedules communication based on the global network topology. This requires a topology-gathering phase followed by a scheduling phase. In order to acquire the network connectivity graph, we aggregate the neighbor lists from each node at the gateway. We then construct connectivity and interference graphs and schedule nodes based on k-hop coloring, such that two nodes with the same slot schedule are mutually separated by at least k+1 hops. Figure 6 shows the impact of node degree on lifetime. As the number of neighbors a node communicates with increases, the number of transmit and receive slots correspondingly increases consuming more energy. In Figure 7(a) we show the connectivity graph of a randomly generated topology with 100 nodes. The graph was colored based on the connectivity to ensure that it is free of collisions. Links can then be removed by instructing an adjacent node to no longer wakeup to listen on that particular timeslot. Using this principle we can reduce the degree of nodes while checking to maintain network connectivity. The reduced degree topology shown in Figure 7(b) reduces the average network energy and simplifies routing. Such logical topology control is not possible with random access protocols.

3.4. Effectiveness of Interference-free Node Scheduling

A major underlying assumption in RT-link is that 2-hop scheduling results in an interference free schedule. Traditionally, TDMA multi-hop wireless scheduling has been solved as a distance-k graph coloring problem, where k is set to be 2. In order to validate this assumption, we tested the interference range of a node with respect to its transmission range. We placed a set of nodes along a line in an open field and measured the packet loss between a transmitter and receiver as the transmitter's distance was varied. Once the stable communication distance between a transmitter and receiver was determined, we evaluated the effect of a

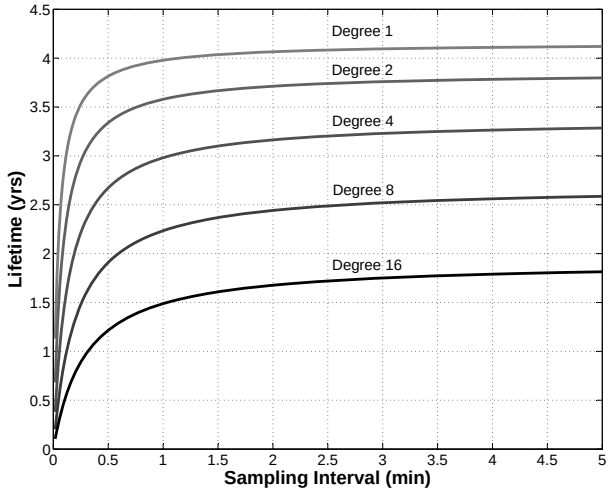

Figure 6: Life given increasing node degree between 1 and 10. Node degree one yields the longest life.

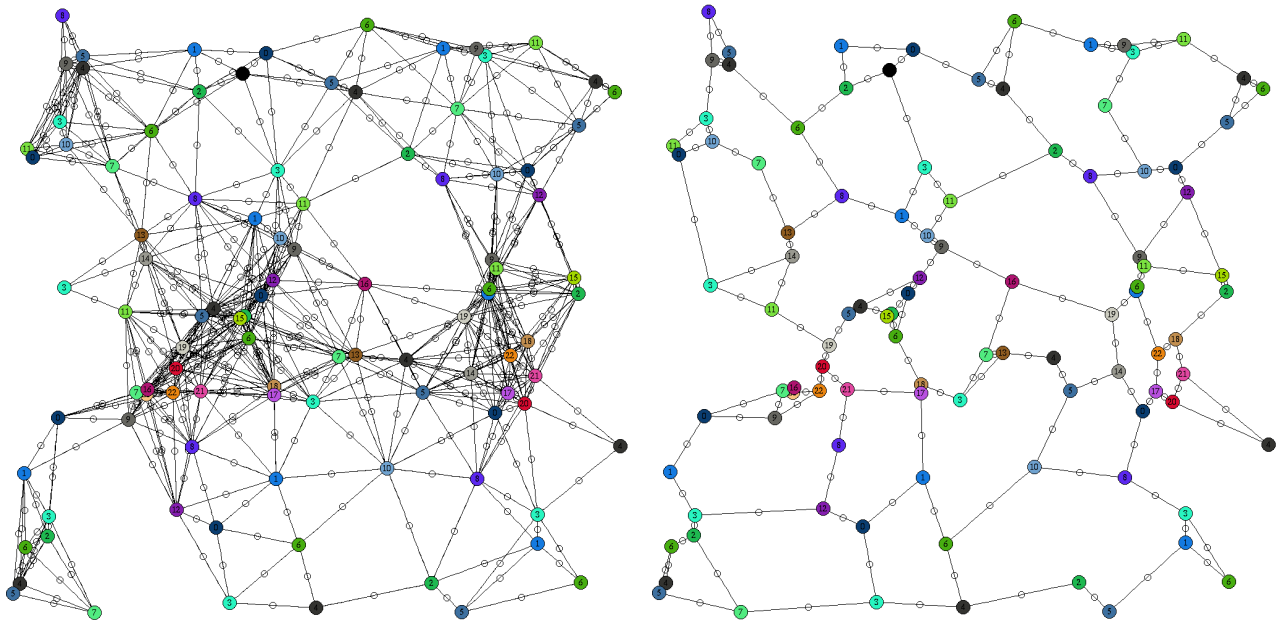

(a) Physical Connectivity Graph.

(b) Pruned Logical Connectivity.

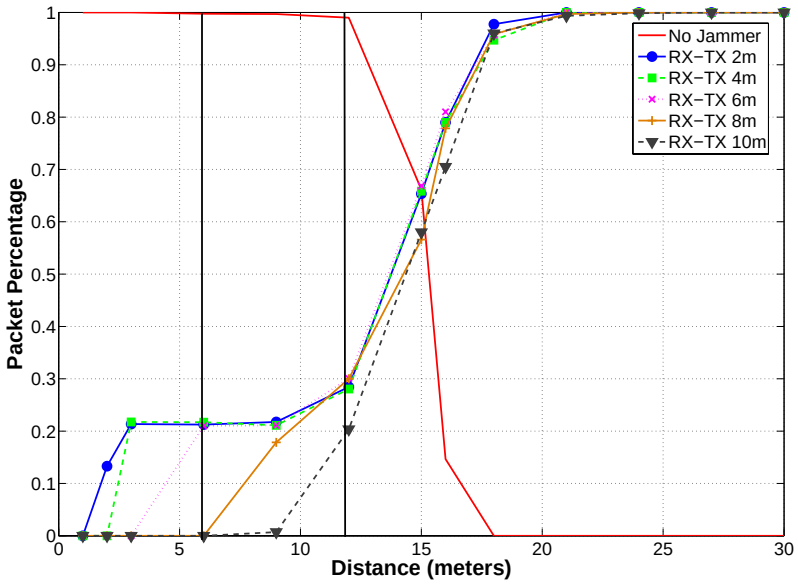

Figure 7: Packet Success rate while transmitting in a collision domain.

constantly transmitting node (i.e. a jammer) on the receiver. Our experimental results for stable transmission (power level 8) are shown in Figure 7. We notice that 100% of the packets are received up to a transmitter-receiver distance of 10m. Following this, we placed the transmitter at a distance of 2, 4, 6, 8, 10 and 12 meters and for each transmitter position, a jammer was placed at various distances. At each point, the transmitter sent one packet every cycle to the receiver for 2000 cycles. We measure the impact of the jammer by observing the percentage of successfully received packets.

We observe two effects of the jammer: First, the effect of the jammer is largely a function of the distance of the jammer from the receiver and not of the transmitter from the receiver. Between 12-18 meters, the impact of the jammer is similar across all transmitter distances. Second, when the transmitter and jammer are close to the receiver, (i.e. under 9m), the transmitter demonstrates a capture effect and maintains an approximately 20% packet reception rate.

The above results show that the jammer has no impact beyond twice the stable reception distance (i.e. 20m) and a concurrent transmitter may be placed at thrice the stable reception distance (i.e. 30m). Such parameters are incorporated by the node coloring algorithm in the gateway to determine collision-free slot schedules.

3.5. Network Scheduling

In multi-hop wireless networks, the goal of scheduling has often been to maximize the set of concurrent transmitters in the network [18]. This is achieved either by scheduling nodes or links such that they operate without any collisions. In the networks considered here, the applications generate steady or low data rate flows but require low end-to-end delay. In Figure 8 we see two schedules, one with the minimal number of timeslots, the other containing extra slots but provisioned such that leaf nodes deliver data to the gateway in a single TDMA cycle. The minimal timeslot schedule maximizes concurrent transmissions, but causes quequeing delays and hence does not minimize the upstream latency of all nodes. By assigning the time slots appropriately in preference to faster uplink and downlink routes, we note that for networks with delay-sensitive data, ordering of slots should take priority over maximizing spatial reuse.

The generation of minimum delay schedules is similar to the distance-two graph coloring problem that

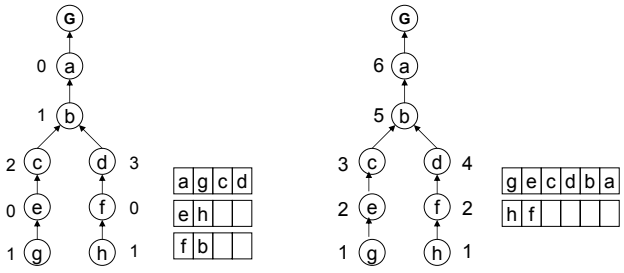

Figure 8: Maximal concurrency schedule (left) compared to a delay sensitive schedule (right). Note that the maximal concurrency schedule needs two frames to deliver all data.

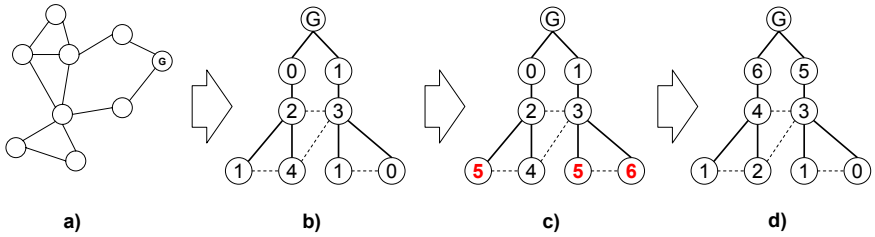

Figure 9: Ordered Coloring to minimize upstream end-to-end delay.

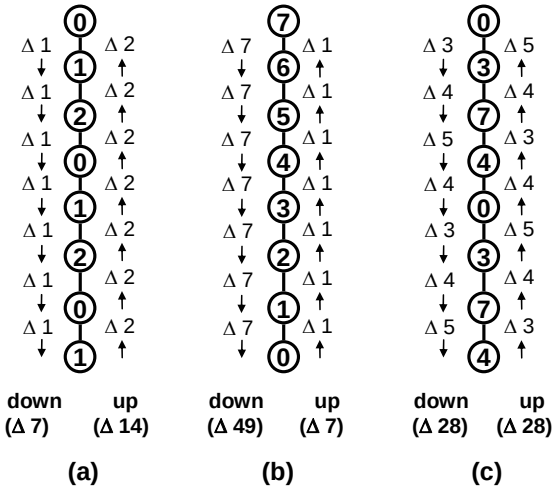

Figure 10: Different schedules change latency based on direction of the flow

is known to be NP-complete [19]. In practice, many heuristics can work well and result in a small constant deviation from the optimal [19]. To illustrate the minimum-delay capability of RT-Link, we briefly discuss one such heuristic to schedule a network where the traffic consists of small packets being routed up a tree to a single gateway. The heuristic consists of four steps. The first step builds a spanning tree over the network rooted at the gateway. Using Dijkstra's shortest path algorithm any connected graph can be converted into a spanning tree. As can be seen in Figure 9(b), the spanning tree must maintain "hidden" links that are not used when iterating through the tree to ensure the 2-hop constraint is still satisfied in the original graph. Once a spanning tree is constructed, a breadth first search is performed starting from root of the tree. The heuristic begins with an initially empty set of colors. As each node is traversed by the breadth first search, it is assigned the lowest value in the color set that is unique from any 1 or 2-hop neighbors. If there are no free colors, a new color must be added into the current set. The next step in the heuristic tries to eliminate redundant slots that lie deeper in the tree by replacing them with larger valued slots. As will become apparent in the next step, this manipulation allows data from the leaves of the tree to move as far as possible towards the gateway in a single TDMA cycle. Figure 9(c) shows how the previous three nodes are given larger values in order to minimize packet latencies. The final step in the heuristic inverts all of the slot assignments such that lower slot values are towards the edge of the tree allowing information to be propagated and aggregated in a cascading manner towards the gateway.

Many applications like interactive voice streaming may benefit from balanced upstream / downstream latency. Figure 10 shows how different scheduling schemes can increase or decrease latency in a line for each flow direction. Figure 10 (a) shows the minimum color schedule for a linear chain with a worst case delay of 31 slots per hop, (b) shows the minimal upstream latency coloring optimized for sensor data collection tasks with a minimum upstream delay of 1 slot, and (c) shows a balanced schedule for bi-directional voice communication with a symmetric delay of 4 slots in either direction. Next to each node, is an arrow indicating the direction of the flow and the number of slots of latency associated with the next hop. A change from a lower slot value to a higher slot value must wait for the next TDMA frame and hence may have a large penalty. We observe that for high end-to-end throughput, minimizing the number of unique slots is essential. The minimum node color schedule in Figure 10 (a), delivers the maximum end-to-end throughput for a chain of nodes assuming the TDMA cycle has only 3 colors, i.e. 1/3 the link data rate. Secondly, we see that for delay-sensitive applications, ordering of the slots is just as important as minimizing the colors. As seen in Figure 10 (c), we use many more colors, but achieve a lower end-to-end delay in both directions then (a) which uses fewer colors.

3.6. Explicit Rate Control

RT-Link allows explicit rate control by specifying a 4-bit rate index r, in the schedule assigned to each node. A flow's rate is defined by the number of active frames that it transmits specified by 2^{r-1}. For example, rate 1 transmits on every frame while rate 3 transmits on every 4th frame. Using this scheme we can vary a flow's rate by control the number of slots and the rate index assigned to it.

3.7. TDMA Slot Mechanics

When a node is first powered on, it activates the AM receiver and waits for the first synchronization pulse. Figure 11 shows the actual timing associated with our TDMA frames. Once the node detects a pulse, it resets the TDMA frame counter maintained in the microcontroller which then powers down the AM receiver. When the node receives its synchronization pulse, it begins the active TDMA time cycle. After checking its receive and transmit masks, the node determines which slots it should transmit and receive on. During a receive timeslot, the node immediately turns on the receiver. The receiver will wait for a packet, or if no preamble is detected it will time out.

The received packet is read from the CC2420 chip into a memory address that was allocated to that particular slot. We employ a zero-copy buffer scheme to move packets from the receive to the transmit

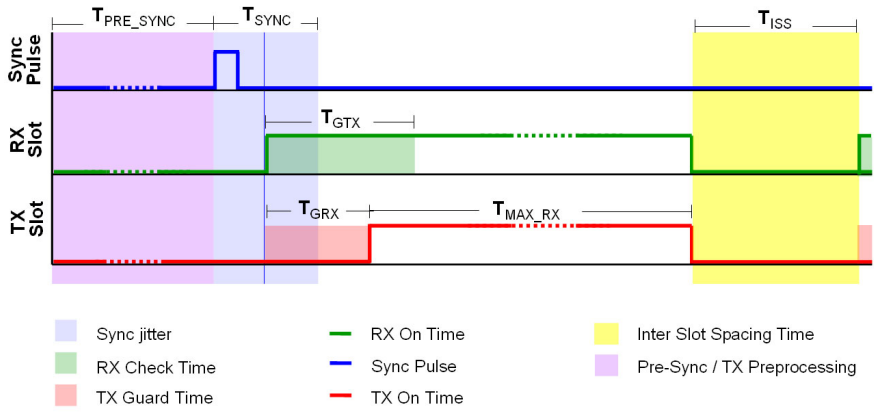

Figure 11: RT-Link operation and timing parameters.

queue. In the case of automatic packet aggregation, the payload information from a packet is explicitly copied to the end of the transmit buffer. When the node reaches a transmit timeslot, it must wait for a guard time to elapse before sending data. Accounting for the possibility that the receiver has drifted ahead or behind the transmitter, the transmitter has a guard time before sending and the receiver preamble-check has a guard time extending beyond the expected packet. Table 3 in the next section shows the different timeout values that work well for our hardware configuration. Once the timeslot is complete, there needs to be an additional guard time before the next slot. We provide this guard time plus a configurable inter-slot processing time that allows the MAC to do the minimal processing required for inter-slot packet forwarding. This feature is motivated by memory limitations and reduction of network queue sizes.

Figure 12 shows a sample trace of two nodes communicating with each other. The rapid receiver checks at the end of the cycle show the contention period with low-power listening for the duration of a preamble.

3.8. Energy Model

To calculate the node duty cycle and lifetime we sum the node's energy consumptions over a TDMA frame. Table 2 shows the power consumed by each component assuming operation at 3 volts. Table 3 and Table 4 show the timing parameters and the energy of each operation during the TDMA frame. The active time of each TDMA slot, T_{active}, is dependent on the total number of slots, N_{slots}, the maximum slots transmit time $T_{max\_payload}$, the AM synchronization setup T_{sync_setup} and capture T_{sync} as well as inter slot processing time T_{ISS}. The number of slots and the length of the TDMA frame are dependent on the desired application sampling rate and throughput configured by the developer.

$$T_{active} = T_{sync\_setup} + T_{sync} + N_{slots} * (T_{max\_payload} + T_{ISS}) \quad (1)$$

The idle time, T_{idle}, between slots is the difference between the active time and the total frame time, T_{frame}. This is typically customized for the specific application since it has impact on both battery life and latency. For long sampling intervals, idle time can be added at the end of the active TDMA slots.

$$T_{idle} = T_{frame} - T_{active} \quad (2)$$

The three customizable parameters that define the lifetime of a node are the TDMA frame time, the number of TDMA slots (including the number of contention slots $N_{contention}$) and the degree d of the node. As the degree increases, the node must check the start of additional time slots and may potentially have to receive packets from its neighbors. The minimum energy that the node will require during a single TDMA frame E_{min} is the sum of the different possible energy consumers assuming no packets are received and the node

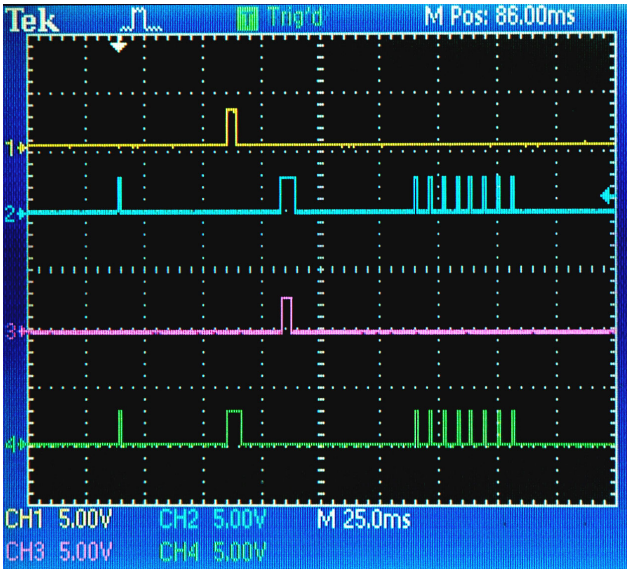

Figure 12: Channels 1 and 2 show transmit and receiver activity for one node. Channels 3 and 4 show radio activity for a second node that receives a packet from the first node and transmits a response a few slots later. The small pulses represent RX checks that timed out. Longer pulses show packets of data being transmitted. The group of pulses towards the right side show the contention slots.

does not transmit packets:

$$E_{min} = E_{sync} + (d + N_{contention}) * E_{GRX} + E_{CPU\_active} + E_{CPU\_sleep} + E_{radio\_idle} + E_{radio\_sleep} \quad (3)$$

The maximum energy the node can consume during a single TDMA frame is the minimal energy consumed during that frame summed with the possible radio transmissions that can occur during a TDMA frame.

$$E_{max} = E_{min} + (d + N_{contention}) * E_{RX} + N_{TX\_slots} * E_{TX} \quad (4)$$

The maximum power consumed by a node over a TDMA frame can be computed as follows:

$$P_{avg} = E_{max}/T_{frame} \quad (5)$$

The lifetime of the node can be computed as follows:

$$Lifetime = (E_{capacity}/E_{max}) * T_{Frame} \quad (6)$$

Figure 6 shows the lifetime of a single node with respect to the sample rate and the number of neighbors. The node in this example is set to operate at the lowest rate that matches the sampling rate interval with no contention slots. As the degree of the node increases, the number of receive checks increase hence decreasing the lifetime. As mentioned before, logical pruning of the topology by selective listening can have a large impact on system lifetime.

3.9. Lifetime

Two major factors control node lifetime in sensor networks are the topology and event sampling rate. We have already shown how RT-Link allows for logical pruning of topology to conserve energy. We will now investigate the lifetime with respect to event sampling rate. A typical LPL-CSMA approach must balance long preamble transmit times with the frequency of channel activity checks. As described in [4] we observe

Power Parameters	Symbol	I(ma)	Power(mW)
Radio Transmitter	P_{radio_TX}	17.4	52.2
Radio Receiver	P_{radio_RX}	19.7	59.1
Radio Idle	P_{radio_idle}	0.426	1.28
Radio Sleep	P_{radio_sleep}	$1e^{-3}$	$3e^{-3}$
CPU Active	P_{CPU_active}	1.1	3.3
CPU Sleep	P_{CPU_sleep}	$1e^{-3}$	$3e^{-3}$
AM Sync Active	P_{sync}	5	15

Table 2: Power Consumption of the main components.

Timing Parameters	Symbol	Time (ms)
Max Packet Transfer	$T_{max\_payload}$	4
Sync Pulse Jitter	T_{sync}	$100e^{-3}$
Sync Pulse Setup	T_{sync_setup}	$20 + (\rho * T_{frame})$
RX Timeout	T_{GRX}	$300e^{-3}$
TX Guard Time	T_{GTX}	$100e^{-3}$
Inter Slot Spacing	T_{ISS}	$500e^{-3}$
Clock Drift Rate	ρ	$10e^{-2}s/s$

Table 3: Timing Parameters for main components.

Energy Parameters	Symbol	Energy (mW)
Synchronization	E_{sync}	$P_{sync}*$ $(T_{sync} + T_{sync\_setup})$
Active CPU	E_{CPU_active}	$P_{CPU\_active} * T_{active}$
Sleep CPU	E_{CPU_sleep}	$P_{CPU\_sleep} * T_{idle}$
TX Radio	E_{radio_tx}	$P_{radio\_tx}*$ $(T_{max\_payload} + T_{GTX})$
RX Radio	E_{radio_rx}	$P_{radio\_rx} * T_{max\_payload}$
Idle Radio	E_{radio_idle}	$P_{radio\_idle} * T_{active}$
Sleep Radio	E_{radio_sleep}	$P_{radio\_sleep} * T_{idle}$
RX Radio Check	E_{GRX}	$P_{radio\_rx} * T_{GRX}$

Table 4: Energy of components with respect to power and time.

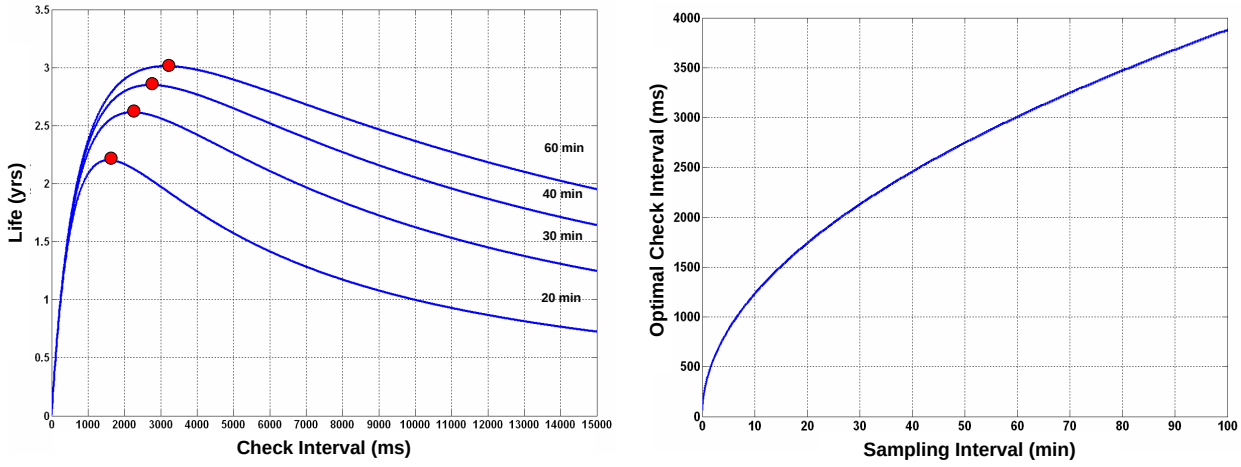

(a) LPL CSMA Check Rate vs Life at 30 min sample interval

(b) Sample Interval vs Optimal Check Rate

Figure 13: Effect of Sample Interval on LPL CSMA Check Rate

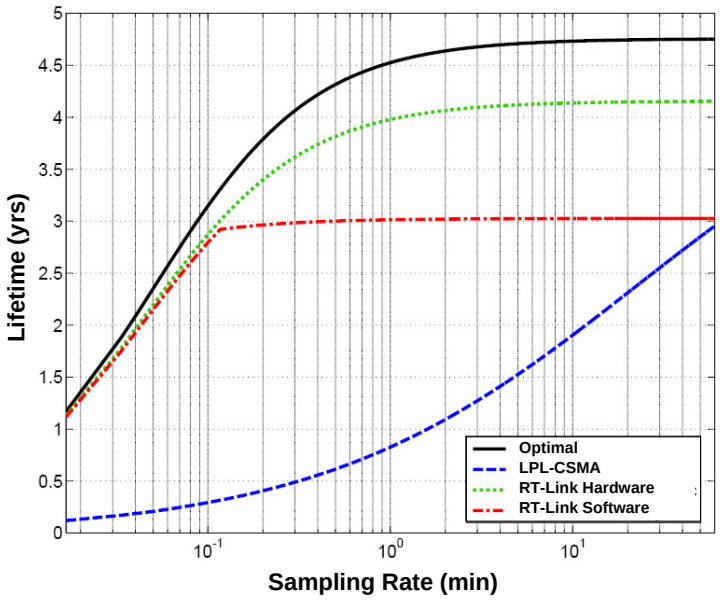

Figure 14: Sample Interval vs Lifetime for both CSMA and TDMA.

Parameter	**Symbol**	**Value**
Sleep Power	P_{sleep}	$90mW$
Sample Time	T_s	
Check Interval	T_c	
Channel Check Time	T_{cca}	$2.5ms$
Sample Energy	E_{sample}	$150mJ$
Battery Capacity	C_{bat}	$2500mAh$
Voltage	V	3.0

Table 5: LPL-CSMA parameters.

a curve similar to Figure 13(a) where at a given sampling rate, there is an optimal lifetime produced by a particular check rate. The authors in [4] neglected to include the voltage when calculating power and hence their lifetimes where exaggerated. We show the corrected graph using power values based on our hardware. The lifetime can be computed in (8).

$$E_{idle} = P_{sleep} * (T_s - (T_{cca} * \frac{T_s}{T_c})) \tag{7}$$

$$L = C_{bat} / \frac{(\frac{T_s}{T_c} * E_{sample}) + (T_c * P_{tx}) + E_{rx} + E_{cpu} + E_{idle}}{T_s * V * 24 * 365} \tag{8}$$

Table 5 describes the above values where L is the node lifetime in years. For a given sampling rate, checking the channel more or less frequently can be quite inefficient. In a multi-hop environment, this means that for a particular event rate of interest, the end-to-end latency is a function of the system check rate which must be fixed in order to achieve the optimal lifetime. This implies that without time synchronization, large sampling intervals will lead to longer latencies. Figure 13(b) shows the optimal check rate as a function of the sampling rate. This is determined by taking the zero of the derivative of equation 8 for every sampling rate. The dot represents the optimal check rate at the 30 minute sampling rate from the previous graph. Here we see that even as the event rate approaches 100 minutes, the check rate must still be less than 4 seconds

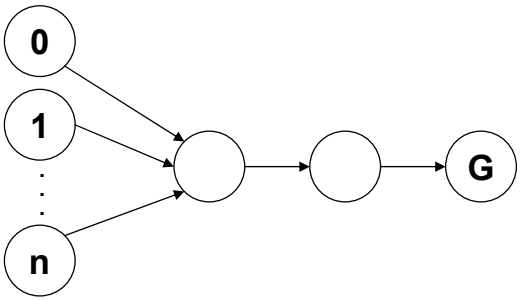

Figure 15: Multi-hop network topology with hidden terminal problem.

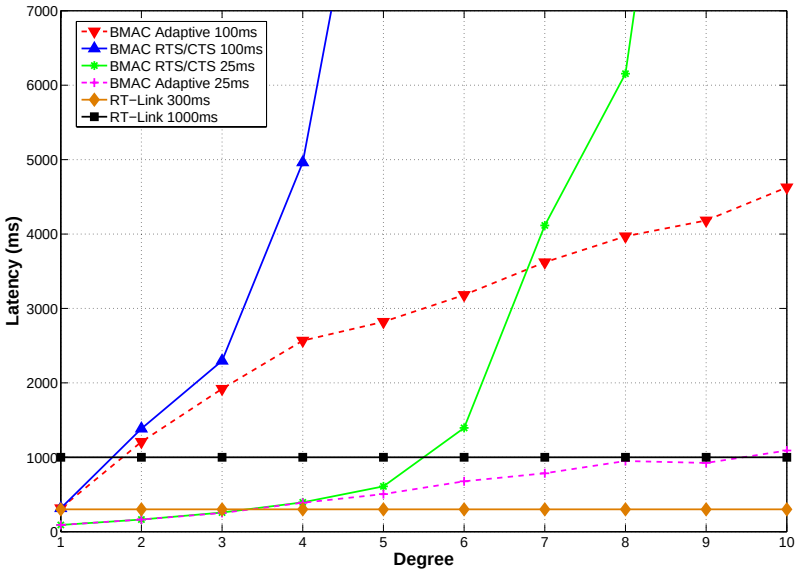

Figure 16: Impact of Latency with node degree

to achieve the best lifetime. In that period of time with a single neighbor, approximately 1500 checks would have gone wasted. Figure 3.8 shows sampling rate with respect to lifetime for RT-link (with and without hardware time synchronization), the optimal node lifetime and the optimal LPL-CSMA lifetime. The overall optimal lifetime assumes perfect node synchronization meaning that the only energy to be consumed is the minimum number of perfectly coordinated packet transmit and receives and the system idle energy. The LPL-CSMA line represents the lifetime given the optimal check rate. We see that for fast sampling rates, hardware time synchronization makes less of a difference. This is because synchronization can be achieved by timing the arrival of normal data messages that already contain slot information. As the sampling rate increases, extra messages must be sent to maintain in-band time synchronization. We see that across the range of a few seconds to nearly two hours, RT-Link with hardware synchronization is quite close to the optimal lifetime and out performs the LPL-CSMA mac protocol by a significant margin.

3.10. End-to-end Latency

In order to investigate the performance of RT-Link, we simulated its operation to compare the end-to-end latency with asynchronous and loosely synchronized protocols across various topologies. To study the latency

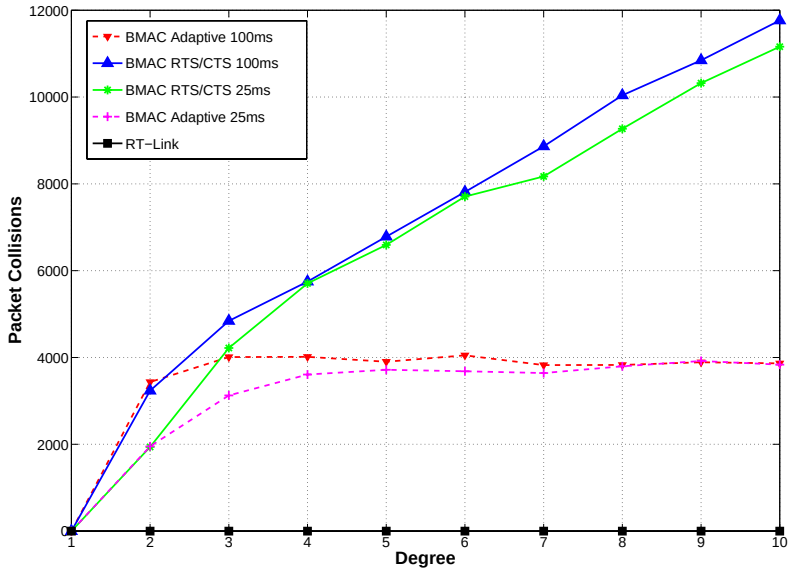

Figure 17: Effect of node degree on collisions for B-MAC

in a multi-hop scenario we focused on the impact of the hidden terminal problem on the performance of B-MAC and S-MAC. All the tests in [4] were designed to avoid the hidden terminal problem and essentially focused on extremely low-load and one-hop scenarios. We simulated a network topology of two "backbone" nodes connected to a gateway. One or more leaf nodes were connected to the lower backbone node as shown in Figure 15. Only the leaf nodes generated traffic to the gateway. The total traffic issued by all nodes was fixed to 1000 1-byte packets. At each hop, if a node received multiple packets before its next transmission, it was able to aggregate them up to 100-byte fragments. The tested topology is the base case for the hidden terminal problem as the transmission opportunity of the backbone nodes is directly affected by the degree of the lower backbone node.

We compare the performance of RT-Link with a 100ms and 300ms cycle duration with RTS-CTS enabled B-MAC operating with 25ms and 100ms check times. The RTS-CTS capability was implemented as outlined in [4]. When a node wakes up and detects the channel to be clear, RTS and CTS with long preambles are exchanged followed by a data packet with a short preamble. We assume B-MAC is capable of perfect clear channel assessment, zero packet loss transmissions and zero cost acknowledgement of packet reception. We observe that as the node degree increases (Figure 16), B-MAC suffers a linear increase in collisions, leading to an exponential increase in latency. With a check time of 100ms, B-MAC saturates at a degree of 4. Increasing the check time to 25ms, pushes the saturation point out to a degree of 8. Using the schedule generate by the heuristic in Section 3.5, RT-Link demonstrates a flat end-to-end latency.

The clear drawback to a basic B-MAC with RTS-CTS is that upon hidden terminal collisions, the nodes immediately retry after a small random backoff. To alleviate problem, we provided nodes with topology information such that a node's contention window size is proportion to the product of the degree and the time to transmit a packet. As can be seen in Figure 17, this allows for a relatively constant number of collisions since each node shares the channel more efficiently. This extra backoff, in turn increases latency linearly with the node degree. We see that RT-Link suffers zero collisions and maintains a constant latency.

4. Nano-RK: A Resource Centric RTOS for Sensor Networks

The push provided by the scaling of technology and the need to support increasingly complicated and diverse applications has resulted in the need for traditional multitasking operating system (OS) abstractions and programming paradigms. The case for small-footprint real-time OS support in sensor networks is strengthened by the fact that many sensor networking applications are time-sensitive in nature i.e. the data must be delivered from the source to the destination within a timing constraint. For example, in a surveillance application, data relayed by a task which is responsible for detecting intruders and subsequently alerting the gateway nodes of the system should be able to reach the gateway on a timely basis. In this section, we present NanoRK, a small-footprint embedded real-time operating system with networking support.

NanoRK supports the classical operating system multitasking abstractions allowing sensor application developers to work in a familiar paradigm resulting in small learning curves, quicker application development times and improved productivity. We show that an efficient implementation of such a paradigm is practical. We associate tasks with priorities and support priority-based preemption i.e, a task can always be preempted by a higher-priority task that becomes eligible to run. For timing sensitive applications, we use priority-based preemptive scheduling to implement the rate-monotonic paradigm [20] of real-time scheduling so that a periodic sensor task set with timing deadlines can be scheduled such that their timing guarantees are honored. Since modern sensor networks use ad-hoc multihop wireless networking for packet relaying, we provide port-based socket abstractions that can be used by sensing tasks for sending and receiving data.

Since sensor nodes are resource-constrained and energy-constrained, we provide functionality whereby the operating system can enforce limits on the resource usage of individual applications and on the energy budget used by individual applications and the system as a whole. In particular, we implement CPU reservations and Network Bandwidth reservations wherein dedicated access of individual application to system resources is guaranteed by the OS. The OS also implements sensor reservations to enforce usage on the number of accesses to individual sensors. Since the energy used by each task is the total sum of energy consumed by the CPU, the radio interface and the individual sensors, a particular setting for each of these leads to an energy reservation. Since we use a static design-time approach for admission control, we provide tools for estimating the energy budget of each application and (hence) the system lifetime. The CPU , network and sensor reservation values of tasks can be iteratively modified by the system designer until the lifetime requirements of the node are satisfied.

4.1 Current Sensor Network Operating Systems

Infrastructural software support for sensor networks was introduced by Hill et al. in [21]. They proposed TinyOS, a low footprint operating system that supports modularity and concurrency using an event-driven approach. TinyOS supports a cyclic-executive model wherein interrupts can register events, which can then be acted upon by other non-blocking functions. We believe that there are several drawbacks to this approach. The TinyOS design paradigm is a significant departure from the traditional programming paradigm involving threads, making it less intuitive for application developers. In contrast, we support a traditional multitasking paradigm retaining task abstractions and multitasking. Unlike TinyOS, where tasks cannot be interrupted, we support priority-based preemption. NanoRK provides timeliness guarantees for tasks with real-time requirements. We provide task management, task synchronization and high-level networking primitives for the developers use. While our footprint size and RAM requirements are larger than that of TinyOS, our requirements are consistent with current embedded microcontrollers. Sensor network hardware typically has ROM requirements of 32-64 KB and RAM requirements of 4-8 KB. NanoRK is optimized primarily for memory and secondarily for ROM. SOS [22] is architecturally similar to TinyOS with the additional capability for loading dynamic run-time modules. In contrast to SOS, we propose a static, multitasking paradigm with timeliness and resource reservation support.

The Mantis OS [23] is the most closely related work to ours in the existing literature. In comparison to

Mantis, we provide explicit support for periodic task scheduling that naturally captures the duty cycles of multiple sensor tasks. We support real-time tasksets that have deadlines associated with their data delivery. We use the novel mechanisms of CPU and network reservations to enforce limits on the resource usage of individual tasks. With respect to networking we provide a rich API set for socket-like abstractions, and a generic system support for network scheduling and routing. NanoRK is power-management and provides several power-aware APIs that can be used by the system. [1]

While low footprint operating systems such as uCOS and Emeralds [24] support real-time scheduling, they do not have support for wireless networking. Our networking stack is significantly smaller in terms of footprint as compared to existing implementation of wireless protocols like Zigbee (around 25 KB ROM and 1.5 KB RAM) and Bluetooth (around 50KB ROM). We also provide high-level socket-type abstractions, and hooks for users to develop or modify custom MAC protocols.

Our system infrastructure can be used to complement distributed sensor applications such as an energy efficient surveillance system [25] and [26]. Our contributions are orthogonal to the literature on real-time networking / resource allocation protocols [27, 28], energy-efficient routing/ scheduling schemes [29, 5] , data aggregation schemes [30], energy efficient topology control [31] and localization schemes [32, 33]. Our OS can be used as a software platform for building higher-layer middleware abstractions like [34]. Our energy reservation mechanism can be used to prevent the type of energy DoS attacks described in [35].

Finally, our work complements [36] in extending the resource kernel paradigm to energy-limited resource-constrained environments like sensor networks.

4.2. Design Goals for a Sensor Networking RTOS

We present the following design goals for an RTOS targeting wireless sensor networks.

- **Multitasking:** The OS should provide a simple and intuitive programming paradigm for easy use by application developers. It is desirable to retain the traditional multitasking paradigm familiar to both desktop and embedded system programmers. Application developers should be able to concentrate on application logic rather than low-level system issues such as scheduling, and networking.

- **Networking Stack Support:** The OS should support multihop networking, routing and simple user-level networking abstractions similar to sockets. In particular, low-level networking details such as reliable packet transmission, multicasting, queue management etc. should be handled by the OS.

- **Support for Priority-based Preemption:** Node battery lifetime continues to be a major challenge in sensor networks. Hence, given that energy consumed by processing per bit is significantly less than the per-bit energy consumed by the radio interface, there is a trend toward increased local processing (such as embedded vision and sound processing). This typically results in increased task execution times. In such situations where task run-times are large, there is a need for priority-based preemption to give precedence to higher priority events.

  True preemptive multitasking becomes necessary in a system where multiple inputs to the system must be serviced at different rates within a required period. For instance, imagine a sensing platform consisting of a microphone, light sensor, radio interface, a GPS for position information or time synchronization and a smart camera system. Figure Table 6 shows typical period and execution times for each of these devices. Manually scheduling such a task set can become daunting using timer interrupts.

  A non-preemptive scheme might handle the radio with an external interrupt, the light and microphone with two priority-based timers, and leave the GPS and camera processing for the main program loop. Even in this situation, the developer may encounter difficulties because the camera servicing time

[1] Power-aware APIs can also be used by applications, albeit with prudence.

	Period	Execution Time
Radio	Sporadic	10 ms
Microphone	200 hz	10 us
Light Sensor	166 hz	10 ms
Smart Camera	1 hz	300 ms
GPS	5 hz	10 ms

Table 6: A sample task set with update periods and execution times.

is longer than the period of the GPS. Given that many low-end microcontrollers have limited timer interrupts, it can become difficult to schedule such a task set. Developers may need to resort to manual time splicing of their functions, thus making future modifications difficult. With a preemptive priority-based system, each of these sensing functions would be supported by a prioritized periodic task.

- **Timeliness and Schedulability:** Most sensor applications such as surveillance tend to be time-sensitive in nature where packets must be relayed and forwarded on a timely basis. While routing and network link scheduling are important components in ensuring that packets meet their end-to-end delay bounds, timing support on each node in the network is also essential. In order to honor end-to-end deadlines, local tasks on each node have deadlines associated with the completion of their local data relaying and processing. Managing the deadlines of these tasks requires support of a *real-time* operating system.

- **Battery Lifetime Requirements:** Guaranteeing sensor node battery lifetimes of 3 to 5 years continues to be a major challenge in sensor networks. If limits on the usage of energy can be enforced, lifetime guarantee requirements of the system as a whole can likely be provided (under reasonable assumptions about operating conditions such as network connectivity). The OS can also ensure that the system energy is apportioned in a manner commensurate to the importance of the tasks so that critical tasks are guaranteed their energy budget.

- **Enforcement of Resource Usage Limits:** Since sensor nodes are resource-constrained, precious CPU cycles, network buffers and bandwidth should be apportioned to application needs. OS support for guaranteed, timely and limited access to system resources is necessary for supporting application deadlines and balanced apportioning of system slack (residual unused resources). This mechanism can also be used to place some limits on the impact of faulty or malicious tasks on system operation.

- **Unified Sensor Interface Abstraction:** Providing a unified and simple abstraction for accessing sensor readings and actuating responses would greatly benefit the end-user. In particular, low-level details associated with sensor/actuator configurations should be abstracted away from the user. Sensors should be supported using device drivers that can return real-world units as well as raw ADC values.

- **Small Footprint:** The current trend of low-end embedded processors is toward larger ROM sizes (64KB to 128 KB) and smaller RAM sizes(2KB to 8KB). The OS architecture should be compliant with this trend by optimizing for RAM with a higher priority than ROM and optimizing for runtime efficiency. This memory constraint also implies that when the choice exists, one prefers a static configuration to a dynamic decision that requires additional data storage and run-time manipulations.

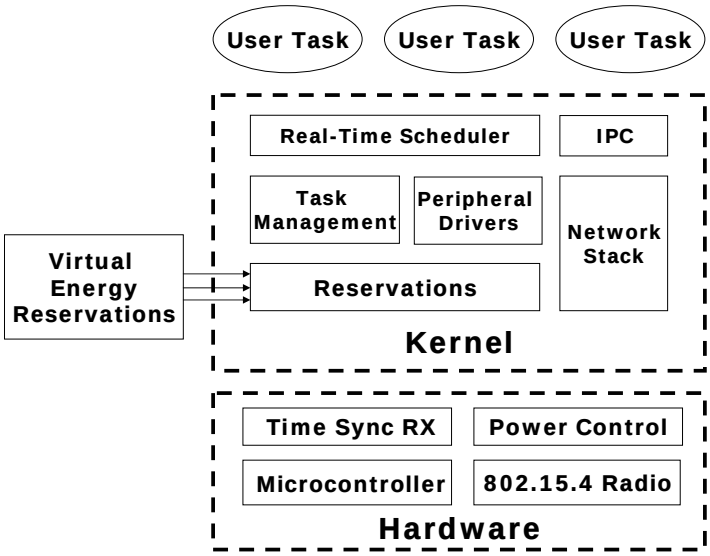

Figure 18: NanoRK Architecture Diagram.

4.3. NanoRK Architecture

The particular requirements of systems support in sensor networking that were discussed earlier impose unique challenges with respect to designing an RTOS. In this section, we describe the architecture of NanoRK, its constructs and capabilities. The overall system architecture of NanoRK is shown in Figure Figure 18.

4.3.1. Static Approach

Given the memory constraints of embedded sensor operating systems, NanoRK uses a static design-time framework. This approach is consistent with sensor networking assumptions because as compared to traditional operating systems (where processes can be dynamically spawned), the OS and the applications are co-located in a single address space. In particular, admission control and real-time schedulability analysis tests are carried out offline as compared to taking a dynamic online approach. We would like to stress that a static approach does not mean that task properties and configuration parameters cannot be reconfigured during run-time. Rather, a static approach enforces the checks to ensure that the dynamic reconfiguration does not adversely affect application and system guarantees in a pre-deployment offline setting as compared to running dynamic admission control algorithms. Data (or control) dependent modifications to the task code such as changing task periods, resource usage limits, resource priorities and configuration of various parameters such as the network buffer sizes and stack sizes of each task can be changed to accommodate mode changes. With current energy and memory constraints, the run-time configurations will need to be verified offline at design-time. [2] This results in light-weight operating system with a small footprint while retaining the rich set of functionality found in conventional RTOSs.

4.3.2. The Reservation Paradigm

The reservation paradigm, as implemented in a *resource kernel* [36], is a simple practical paradigm for guaranteeing timeliness and enforcing temporal isolation in real-time operating systems. Reservation-based resource kernels provide support wherein applications can specify timeliness and resource requirements to the OS, and the OS enforces guaranteed access to system resources so that the application timeliness

[2] Future revisions of NanoRK may relax this constraint.

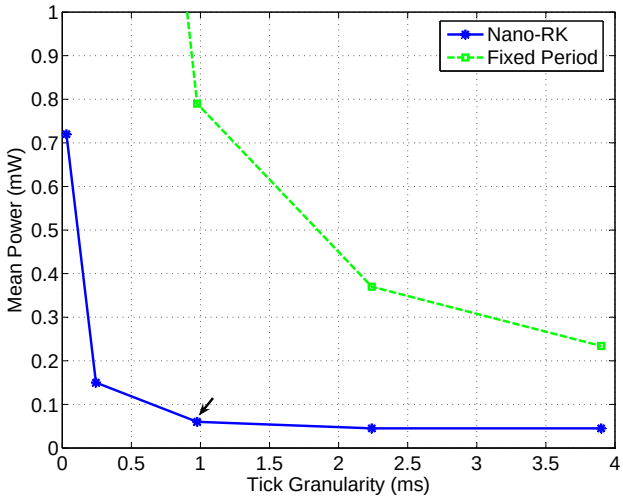

Figure 19: Power Consumption vs Timer Granularity.

requirements are honored. While the resource kernel abstraction has hitherto been used in dynamic run-time settings, the resource reservation paradigm is desirable for static settings as well. A sensor application task can specify its requirement of CPU cycles, network bandwidth and network buffers over fixed periods which will be enforced by the NanoRK kernel. Only tasks that have not depleted their reservation quota rates are eligible for scheduling. In deference to the stringent constraints of sensor nodes, exactly a single task can be associated with a reservation. In contrast, the classical resource kernel concept allows for zero, one or more tasks to be bound to a reservation.

In summary, NanoRK supports CPU reservations, sender/receiver network bandwidth reservations and sensor/actuator reservations. All of these reservations can be combined to enforce a virtual node-wide (and even system-wide) energy reservation.

4.3.3. Energy Management Support

Since maximizing battery lifetime continues to be a major challenge in sensor networks, there is a need for aggressive power savings by operating at low duty cycles. NanoRK enforces this in the form of *virtual energy reservations*. Note that the energy consumed by a task is the total sum of the CPU energy, radio interface energy and the energy associated with turning on sensors and actuators. The CPU and radio energy consumed by the task can be adjusted exactly by changing the CPU and network reservation sizes. In order to bound the energy consumed by sensors, NanoRK provides *sensor reservations*. Our unified sensor interface provides functionality wherein sensors are turned off (gated) by default and any access to a sensor is an atomic operation that consists of the sensor being turned on, its value being read and then being turned off again. This makes it possible for the operating system to set an upper limit on the number of accesses made to a sensor over a particular period. Thus it is is possible to map a resource tuple of $(CPU, Network, Sensor)$ reservations to a particular power level. Given periodic tasks, one can calculate the mean power used by all tasks over a hyper-period, giving a reasonably accurate estimate of the node lifetime. By modifying the values of the $(CPU, Network, Sensor)$ reservation-tuple, the mean energy consumed by each task can be varied. This can be used for either controlling the node lifetime or for varying the proportion of system energy alloted to each task (for example, certain mission critical tasks can be allocated a high energy budget). We again note that energy reservations is implemented by controlling the $(CPU, Network, Sensor)$ reservation-tuple at a pre-deployment stage. This is consistent with the predominantly static approach that NanoRK adopts.

Nano-RK employs a novel energy-efficient time management scheme using one-shot timer interrupts instead of a polling interrupt. Traditionally, an operating system will periodically call the scheduler in order to check if a context swap should occur and to update the time of day (TOD) counter. This consumes excess energy especially during long periods of sleep. Nano-RK operates the main hardware timer in a one-shot mode wherein the next timing interrupt is triggered when either a task is scheduled to be awakened because of an event or because it becomes eligible for scheduling. This is inherently more energy-efficient than schemes that needlessly call the scheduler. Smaller OS tick granularity requires that the hardware interrupt counter be able to accumulate larger values before it overflows. In the case of extended idle intervals, this timer overflow maintenance has an associated energy penalty. Figure 19 shows how timer granularity affects extended idle periods. The top curve shows the average power consumption when the OS periodically calls the scheduler. The bottom curve shows Nano-RK's power consumption using our one-shot timer method. The arrow marker shows Nano-RK's default operating point which allows for better than 1ms timer resolution for use by tasks.

Nano-RK's representation for time is based on the POSIX time structure `timeval`. This consists of two 32-bit numbers to represent the `(seconds,nanoseconds)` fields. The OS TOD counter field is incremented as needed, and overflows will not occur for practically foreseeable intervals of time. This allows Nano-RK to support the fine-granularity timing requirements of real-time applications while maintaining a (practically) non-overflowing notion of absolute time.

4.3.4. Task Management and Scheduling

NanoRK task control block (TCB) structures are populated during initialization[3]. They store the register context of all task (registers and stack), the task's priority, period of recurrence, $(CPU, network, Sensor)$ reservation sizes, port identifiers etc. Two linked lists of TCB pointers are used to order the set of active and suspended tasks respectively, based on period of recurrence. Tasks can block on certain events (such as being woken up at a certain point of time or the arrival of a network packet) and can be unsuspended and enqueued in the OS active list when the events occur. We suspend tasks that have pending events rather than using a polling-based implementation of NanoRK system calls. This is done for energy-efficiency reasons because if there are no tasks eligible to run, the system can be powered down to sleep.

Our system uses priority-based preemptive scheduling and while we provide explicit support for periodic tasks, we also support aperiodic and sporadic tasks in our framework. The highest priority task that is eligible to run in the system is always scheduled by the operating system. A periodic task can suspend itself after the completion of its current instance using the `wait_until_next_period()` system call.

We implement priority ceiling protocol emulation (Highest Locker Priority) to bound the blocking time encountered by a higher priority process due to the phenomenon of priority inversion (wherein a shared resource needed by the high-priority process is currently being used by a lower-priority process). In particular, each mutex is associated with a priority ceiling. When a mutex is acquired (using `lock_mutex()`), the priority of the task is elevated to the priority ceiling of the mutex. Once the mutex is released (using the `unlock_mutex()` system call), the priority of the task reverts to its original level. This results in bounded priority inversion which can be accounted for in the offline schedulability test. Thus, real-time synchronization is supported in NanoRK.

Rather than provide explicit message box support, we provide system support for conventional semaphores that can be used by tasks to manipulate application buffers in a controlled manner for facilitating inter-process communication (using message boxes). This obviates the necessity for OS buffer space for storing message data and allows efficient *zero copying* [37] mechanisms to facilitate information sharing among tasks. Semaphores can also be used as a generalization of mutexes for guarding access to multiple resources.

[3]While we provide API support to modify fields in the TCB during run-time, we encourage static configuration for footprint reduction of the ROM image.

Component	Resource
Context Swap Time	45 μs
Mutex Structure Overhead	5 bytes per resource
Task Stack Overhead	32–128 (typically 64) bytes per task
Task Overhead	30 bytes per task
Link Layer Overhead	200 bytes
2 tasks, 2 mutexes, 2 128-byte network buffers	1KB RAM, 18KB ROM

Table 7: Breakdown of Nano-RK's resource requirements.

4.3.5. Nano-RK Integration with RT-Link

An effective approach to energy-efficient communication is to operate all nodes at low communication duty cycles so as to maximize the shutdown intervals between packet exchanges. The two fundamental challenges in delivering delay-bounded service in such networks are (a) coordinating transmissions so that all active nodes communicate in a tightly synchronized manner and (b) ensuring that all transmissions are collision-free. In Nano-RK, we exploit time synchronization to tightly pack the activity of all nodes so that they may maximize a common sleep interval between activities. Furthermore, in the absence of dropped packets, it provides guarantees on timeliness, throughput and network lifetime for end-to-end communications.

Using global time synchronization, Nano-RK provides a TDMA-based link layer protocol that schedules communication based on the global topology. This requires a topology-gathering phase followed by a scheduling phase. Once the network has been scheduled, communication transactions occur during assigned slots that fit within a periodic set of frames. Thus, a TDMA cycle consists of a finite set of frames each of which repeat a pattern of active and inactive slots.

One challenge associated with this scheme is ensuring that communication still fits within Nano-RK's real-time framework. Rate-Monotonic Analysis [20] specifies a worst-case utilization bound for a task set scheduled with Rate-Monotonic Scheduling as shown in equation 1.

$$U_{rm}(n) = n(2^{1/n} - 1) \tag{9}$$

In the worst case, this approaches $ln(2)$ giving a utilization bound of 69.3%. The utilization of a taskset is calculated as shown in equation 2.

$$\sum_{i=1}^{n} C_i/T_i \tag{10}$$

where C_i is the execution time and T_i is the release period of the task. If the utilization of a given task set is below the theoretical utilization bound, then all tasks will meet their deadlines. We therefore model the communication in our system in such a way that it fits within the Rate Monotonic paradigm.

Individual slots inside each TDMA frame is represented as periodic tasks with execution times equal to a single slot size and a period equal to the frame interval. From the implementation point of view, there is a single link layer task running at the highest priority. This task is given a worst case execution time of the sum of its active slots and a period equal to the frame size. Nano-RK adds the notion of a compound-task which can make a system call that schedules the task before its next period without being subject to undesirable back-to-back scheduling conflicts. An additional reserve can be added such that the task can only operate for a specified CPU reservation (i.e. a single slot time) each time the task is executed (the standard period-based reserve still exists). So while the TDMA communication is modeled as multiple fixed period tasks, in actuality, it executes as a single task with all of the periods composed together.

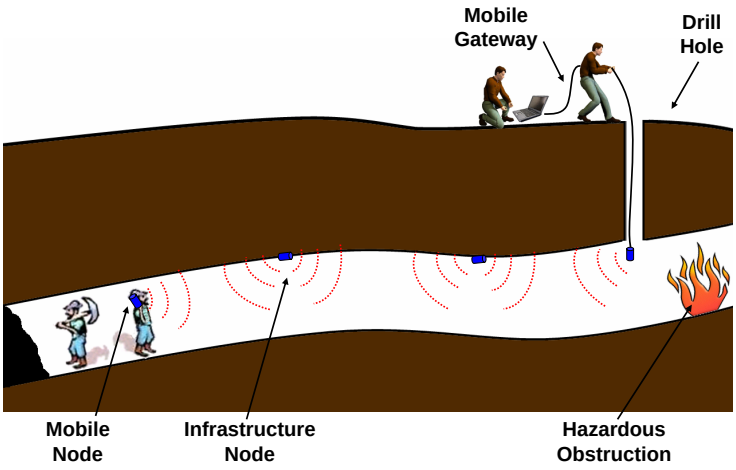

Figure 20: Rescue Sensor Network in Coal Mine

5. Coal Mine Safety Application

Over the past decade, there has been a surge of accidents in coal mines across the world. In most cases, miners are trapped several thousand feet below the surface for several hours while rescuers try to find their location and attempt to communicate with them. In January 2006, 13 miners were trapped for nearly two days in the Sago Coal Mine in West Virginia, USA. The miners were less than few hundred feet from an escape route but were not aware of it. Similarly, in February 2006, in the Pasta de Conchos coal mine in Mexico, 65 miners were trapped more than 1 mile below the ground level. After more than 100 hours of rescue attempts, the authorities were still unable to locate or establish communication with the miners. In both cases, the prevalent wired communication systems were destroyed when a portion of the mine collapsed and there was no way to reestablish connection to the affected areas.

The normal practice to check the status of the trapped miners is to drill a narrow hole (of 1-2 inch radius) from the surface to a mine tunnel and drop a microphone, camera and air quality sensors at different locations around the disaster area. This method provides limited access to the affected region as medium-sized mines may span several miles across. Another method of communicating to the miners is by installing a loop antenna that is several miles long, over the surface of the mine. This scheme uses a low-frequency transmitter on the surface to send one-way broadcasts of short text messages, but is unable to get feedback about the status or location from the miners below.

We propose the establishment of a self-healing wireless network in such mine-like environments to maintain communication in the remaining connected network. If a wireless node was lowered through the drill-hole, it could re-establish communication with the remaining network and initiate two-way communication with the miners. In addition, the miners would be able to leave broadcast voicemail-type messages and allow it to propagate to all nodes in the remaining network.

We were invited to investigate the use of wireless sensor nodes to track miners and to evaluate the viability as an end-to-end rescue communication network for miners during an incident. It is important to note that during normal operation, the network's primary task is to track miners and record environmental-quality data. In order to keep normal network maintenance costs low, it is necessary to meet the following design goals:

1. All nodes are to be battery powered.

2. Nodes must have a predictable lifetime of at least one year under normal operation.

3. Nodes must provision continuous voice communication for at least one week with fully-charged batteries.

4. Voice communication must include two-way interactive calling, one-way "push-to-talk" voice messaging and support for store and broadcast voicemail messaging.

5. The network must be able to tolerate topology changes and self-heal to maintain connectivity after a partition.

We preformed two sets of experiments in the National Institute for Occupational Safety and Health (NIOSH) experimental coal mine facility. The goal of the first deployment was to track the location of mobile nodes carried by miners as well as monitor an assortment of sensors over a period of three weeks. The second deployment was to test an emergency mode of operation where interactive two-way voice is streamed over the network.

5.1. Location Tracking

For our location tracking tests, we deployed 42 nodes across almost 2miles of underground corridors. Every 20 seconds each infrastructure nodes would send a neighbor list with signal strength values for each link as well as the most recent sensor data back to the gateway. As the mobile node moves through the mine, it is added to the different neighbor lists of infrastructure nodes that it passes. This allows for a mobile node to be localized to the nearest access point with the required signal strength information to provide finer localization granularity in the future. Figure 21 shows a map of the coal mine with the overlaid network topology. We see that due to the remaining coal pillars, the degree of the network graph is quite low (at most 5), but the depth is quite large (over 15 hops). Long linear chains can be problematic for in-band time synchronization due to the increasing probability of packet loss across the multiple hops. Since coal miners require power at the face of the mine, there is typically a main power line fed into the mine that is ideal for our AM transmitter. Any nodes located on the main corridor can use the AM time synchronization while nodes on the periphery can use in-band time synchronization. We left the nodes for three weeks logging data every 20 seconds. We found that a few nodes located far away from the AM time synchronized region of the network experienced problems due to dropped packets that lead to higher than normal power consumption. During the network setup we saw that all nodes had reliable links. Narrow passageways, miners and machinery increase packet loss by blocking line of site communication. We gain two lessons from this deployment. First, even in controlled environments link quality can change due to motion in the environment and unforeseen perturbations over time however the topology will return to a steady state. Second, as hop length increases, reliability decreases which causes time synchronization degradation and increased energy consumption in the form of extended synchronization wait times. This indicates that we should further explore how to address link faults in an energy efficient manner.

5.2. Voice Streaming

In our second deployment, we wanted to add the ability for the network to switch into a high rate of operation capable of streaming interactive voice from a gateway to a mobile node. Under normal circumstances, sensor data is collected once every twenty seconds from all nodes. This includes light, temperature, average energy level, battery voltage and the snr values associated with any nearby mobile nodes. During the audio streaming mode of operation, the network would send compressed voice data at 13Kbps. Our primary focus was on the networking and evaluating the feasibility of such a system. For our tests, the mobile node was able to sample audio from the on-board microphone and compress the data while running the networking task. Our current mobile nodes do not have an onboard DAC and speaker output, so we used a laptop connected to the node with a serial port to playback the received audio. To simplify tests, we transferred the raw packet data over the UART and performed the decompression and playback live on the PC. In a next

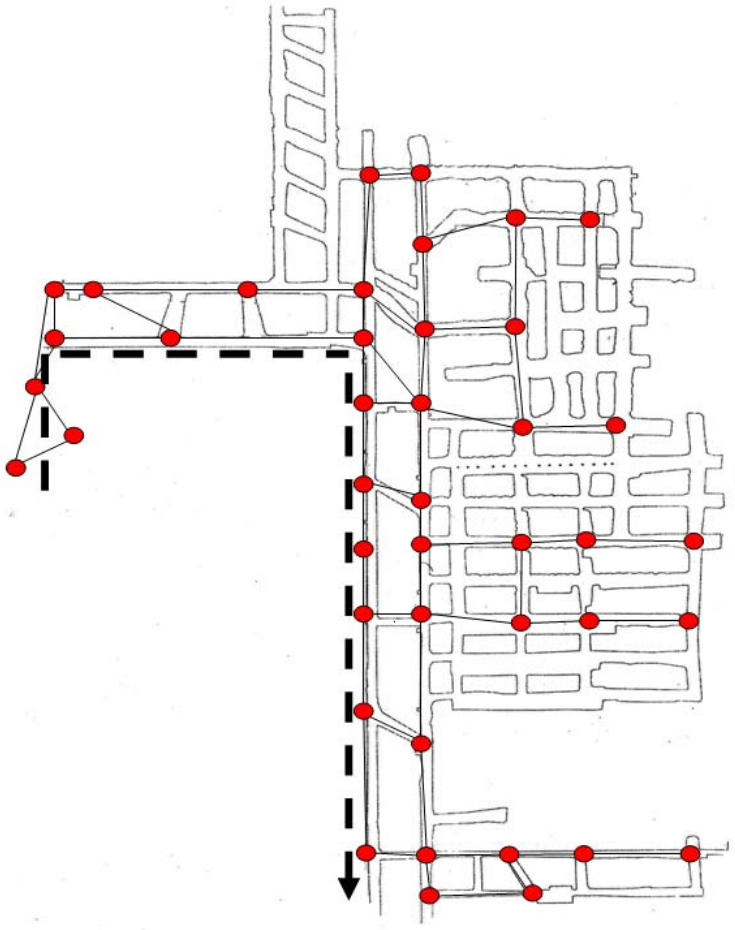

Figure 21: Coal mine map with network topology. Dotted line shows leaky feeder time synchronization cable.

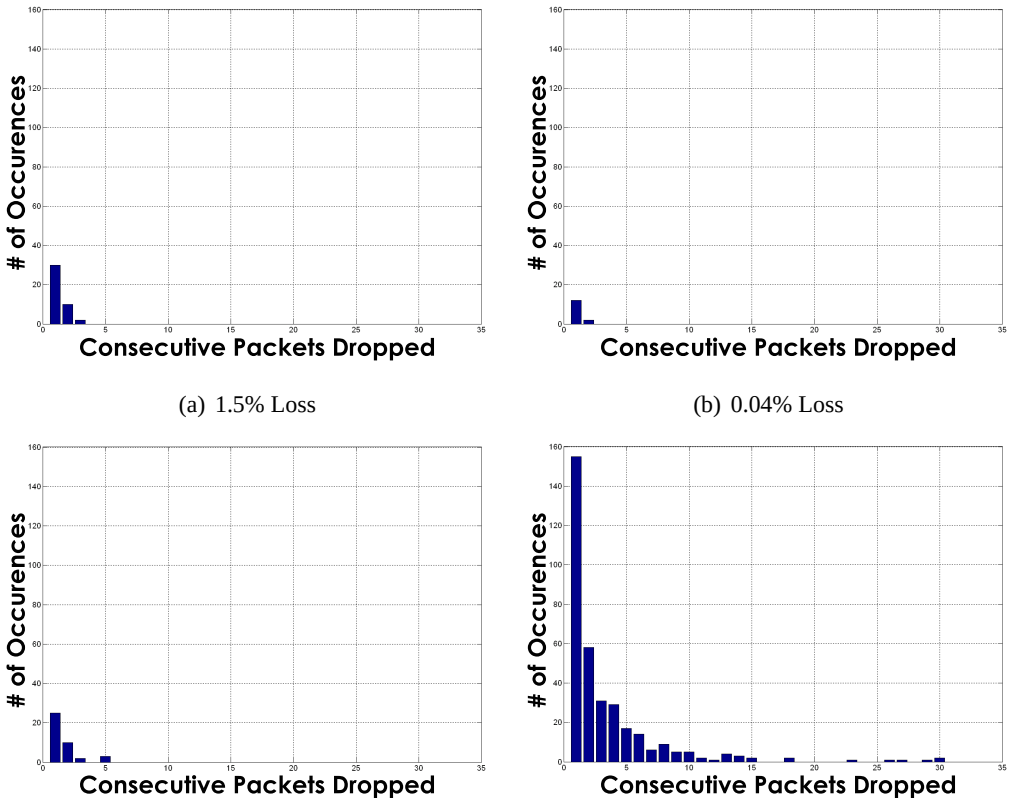

(a) 1.5% Loss

(b) 0.04% Loss

(c) 2.1% Loss

(d) 52.3% Loss

Figure 22: Packet Loss Clustering At Four Points in a Multi-hop Chain of Nodes Streaming Audio

generation device, the handheld mobile node would have a higher end microcontroller capable of doing both the compression and decompression with a built in DAC and speaker system.

In controlled environments outside of the mine we found that the system performed with below 3% packet loss per hop. Sending redundant data in separate packets allowed for easily understandable end-to-end voice transfers. Figure 22 shows the distribution of packet loss clustering at four different hops along an eight hop series of nodes inside the coal mine. The end-to-end latency across the eight hops between when audio was sampled and when the playback occured was just under 200ms. Each hop along a pre-scheduled path towards the gateway maintained an average latency of 24ms. We found that while the mine corridor is clear of obstructions the wireless channel shows few packet drops. In some situations when a machine blocks the narrow corridor we see packet loss rates as high as 50%. Under these circumstances, packet drops are heavily clustering making error concealment or recovery difficult. Since occupancy inside a coal mine is relatively sparse (usually less than 5 groups) compared to the mine's size, clear paths are quite common. Future work will investigate protocols that use the mesh nature of sensor networks to ameliorate broken links by using alternative paths.

References

[1] Atmel corporation, atmega32 data sheet, 2005.

[2] Chipcon inc., chipcon cc2420 data sheet, 2003.

[3] Radio systems 30w tr-6000 am transmitter data sheet, 2001.

[4] J. Polastre, J. Hill, and D. Culler. Versatile low power media access for wireless sensor networks. *SenSys*, November 2005.

[5] W. Ye, J. Heidemann, and D. Estrin. An energy-efficient mac protocol for wireless sensor networks. *INFOCOM*, June 2002.

[6] T. Dam and K. Langendoen. An adaptive energy-efficient mac protocol for wireless sensor networks. *SenSys*, November 2003.

[7] A. El-Hoiydi and J. Decotignie. Wisemac: An ultra low power mac protocol for the downlink of infrastructure wireless sensor networks. *ISCC*, 2004.

[8] V. Rajendran, K. Obraczka, and J. J. Garcia-Luna-Aceves. Energy-efficient, collision-free medium access control for wireless sensor networks. *Sensys*, 2003.

[9] L.F.W. van Hoesel and P.J.M. Havinga. A lightweight medium access protocol for wireless sensor networks. *INSS*, 2004.

[10] L. G. Roberts. Aloha packet system with and without slots and capture. *SIGCOMM*, 5(2):28–42, 1975.

[11] C. Schurgers, V. Tsiatsis, S. Ganeriwal, and M. Srivastava. Topology management for sensor networks: Exploiting latency and density. *MobiHoc*, 2002.

[12] C. Guo, L. C. Zhong, and J. Rabaey. Low power distributed mac for ad hoc sensor radio networks. *Globecom*, 2001.

[13] J. Elson, L. Girod, and D. Estrin. Fine-grained network time synchronization using reference broadcast. *USENIX OSDI*, 2002.

[14] S. Ganeriwal, R. Kumar, and M. B. Srivastava. Timing-sync protocol for sensor networks. *Proc. ACM Sensys*, 2003.

[15] M. Maroti, B. Kusy, G. Simon, and A. Ledeczi. The flooding time synchronization protocol. *Proc. ACM Sensys*, 2004.

[16] Jerry Zhao and Ramesh Govindan. Understanding packet delivery performance in dense wireless sensor networks. *Proc. ACM Sensys*, 2003.

[17] Anthony Rowe, Rahul Mangharam, and Raj Rajkumar. RT-Link: A Time-Synchronized Link Protocol for Energy-Constrained Multi-hop Wireless Networks. *CMU Tech Report TR05-08*, 2005.

[18] Randolph D. Nelson and Leonard Kleinrock. Maximum probability of successful transmission in a random planar packet radio network. *INFOCOM*, pages 365–370, 1983.

[19] Hari Balakrishnan et al. The distance-2 matching problem and its relationship to the mac-layer capacity of ad hoc wireless networks. *IEEE Journal on Selected Areas in Comm.*, 22(6):1069–1079, August 2004.

[20] C. L. Liu and J. W. Layland. Scheduling algorithms for multiprogramming in a hard real-time environment. *Journal of ACM*, 20(1):46–61, 1973.

[21] Alec Woo Seth Hollar David Culler Kristofer Pister Jason Hill, Robert Szewczyk. System architecture directions for network sensors. *ASPLOS 2000*, November 2000.

[22] Roy S Shea Eddie Kohler Mani B Srivastava Simon Han, Ramkumar Rengaswamy. Sos : A dynamic operating system for sensor nodes. *Mobisys*, June 2005.

[23] J. Carlson H. Dai J. Rose A. Sheth B. Shucker J. Deng R. Han H. Abrach, S. Bhatti. Mantis: System support for multimodal networks of in-situ sensors. *2nd ACM International Workshop on Wireless Sensor Networks and Applications (WSNA)*, 2003.

[24] Pillai P. Zuberi, K. M. and K. G. Sin. Emeralds: A small-memory real-time microkernel. *In Proceedings of the 17th ACM Symposium on Operating System Principles*, June 1999.

[25] John A. Stankovic Tarek Abdelzaher Liqian Luo Radu Stoleru Ting Yan Lin Gu Jonathan Hui Bruce Krogh. Tian He, Sudha Krishnamurthy. Efficient surveillance system using wireless sensor networks. *MobiSys*, June 2004.

[26] Wang Y Martonosi M Peh L-S Rubenstein D Juang P, Oki H. Energy-efficient computing for wildlife tracking: design tradeoffs and early experiences with zebranet. *ACM ASPLOS*, 2002.

[27] Chenyang Lu Lui Sha Jennifer Hou John A. Stankovic, Tarek Abdelzaher. Real-time coomunication and coordination in embedded sensor networks. *Proceedings of the IEEE*, 91(7), July 2003.

[28] Chi-Sheng Shih Simone Giannecchini, Marco Caccamo. Collaborative resource allocation in wireless sensor networks. *ECRTS*, pages 35–44, 2004.

[29] Wook Hyun Kwon Hyung Seok Kim, Tarek Abdelzaher. Minimum-energy asynchronous dissemination to mobile sinks in wireless sensor networks. *ACM SenSys*, November 2003.

[30] Ramesh Govindan Chalermek Intanagonwiwat and Deborah Estrin. Directed diffusion: A scalable and robust communication paradigm for sensor networks. *Mobicom*, August 2000.

[31] Jennifer C. Hou Ning Li and Lui Sha. Design and analysis of a mst-based distributed topology control algorithm for wireless ad-hoc networks. *IEEE Trans. on Wireless Communications*, 4(3):1195–1207, May 2005.

[32] Brian Blum John Stankovic Tarek Abdelzaher Tian He, Chengdu Huang. Range-free localization schemes for large scale sensor networks. *Mobicom*, September 2003.

[33] Jennifer C. Hou Wei-Peng Chen and Lui Sha. Dynamic clustering for acoustic target tracking in wireless sensor networks. *Mobicom*, 3(3), July 2004.

[34] Tarek Abdelzaher et al. Envirotrack: Towards an environmental computing paradigm for distributed sensor networks. *IEEE International Conference on Distributed Computing Systems*, March 2004.

[35] A. D. Wood and J. Stankovic. Denial of service in sensor networks. *IEEE Computer*, 35(10):54–62, 2002.

[36] A. Molano R. Rajkumar, K. Juvva and S. Oikawa. Resource kernels: A resource-centric approach to real-time and multimedia systems. *In Proc. of the SPIE/ACM Conference on Multimedia Computing and Networking.*, January 1998.

[37] Hsiao Keng and J. Chu. Zero-copy tcp in solaris. *USENIX*, 1996.